

Electrical creation of spin polarization in silicon at room temperature

Saroj P. Dash¹, Sandeep Sharma¹, Ram S. Patel¹, Michel P. de Jong¹ & Ron Jansen¹

The control and manipulation of the electron spin in semiconductors is central to spintronics^{1,2}, which aims to represent digital information using spin orientation rather than electron charge. Such spin-based technologies may have a profound impact on nanoelectronics, data storage, and logic and computer architectures. Recently it has become possible to induce and detect spin polarization in otherwise non-magnetic semiconductors (gallium arsenide and silicon) using all-electrical structures^{3–9}, but so far only at temperatures below 150 K and in n-type materials, which limits further development. Here we demonstrate room-temperature electrical injection of spin polarization into n-type and p-type silicon from a ferromagnetic tunnel contact, spin manipulation using the Hanle effect and the electrical detection of the induced spin accumulation. A spin splitting as large as 2.9 meV is created in n-type silicon, corresponding to an electron spin polarization of 4.6%. The extracted spin lifetime is greater than 140 ps for conduction electrons in heavily doped n-type silicon at 300 K and greater than 270 ps for holes in heavily doped p-type silicon at the same temperature. The spin diffusion length is greater than 230 nm for electrons and 310 nm for holes in the corresponding materials. These results open the way to the implementation of spin functionality in complementary silicon devices and electronic circuits operating at ambient temperature, and to the exploration of their prospects and the fundamental rules that govern their behaviour.

Inducing spin polarization in a semiconductor can be done efficiently and at reasonable current levels by electrical transfer of spins from a ferromagnetic metal across a thin tunnel barrier, as established using optical detection methods for GaAs^{10,11} and Si at low temperature¹². Spin polarization in n-type semiconductors has been detected in all-electrical devices^{3–9} at low temperature (5–50 K; in a few cases up to 150 K). Electrical spin detection is often done in a lateral non-local geometry^{3,5–7}, where the non-local voltage representing the spin polarization in the semiconductor is typically of the order of 10 μ V. A second scheme^{8,9} uses a single contact for both injection and detection, in a three-terminal geometry (Fig. 1a). We use the latter, single-interface geometry to extract the spin polarization and spin accumulation induced in the semiconductor, the spin lifetime and the variation with temperature, T , and bias voltage, V .

The experiment has three significant features. The first is the electrical injection of a spin-polarized tunnel current from the ferromagnet into the Si, producing an imbalance in the electron population in the Si conduction band or in the hole population in the valence band (see Fig. 1b for n-type Si). This is described by different electrochemical potentials, μ^\uparrow and μ^\downarrow , for the up and down spin directions, respectively, and a spin accumulation, $\Delta\mu = \mu^\uparrow - \mu^\downarrow$. The orientation of the spin polarization is determined by the magnetization direction of the ferromagnet, which is parallel to the interface (that is, in-plane). The spin accumulation is greatest directly underneath the contact and decays with increasing distance from the interface with a certain spin diffusion

length, L_{SD} . The second feature is the controlled reduction of the spin accumulation by means of the Hanle effect (Fig. 2a) in an applied magnetic field, B , perpendicular to the carrier spins in the Si. This causes precession of the spins at the Larmor frequency, $\omega_L = g\mu_B B/\hbar$, where g is the Landé g -factor, μ_B is the Bohr magneton and \hbar is Planck's constant divided by 2π . As a result, the spin accumulation decays as a function of B with an approximately Lorentzian line shape given by $\Delta\mu(B) = \Delta\mu(0)/(1 + (\omega_L\tau)^2)$, where τ is the spin lifetime (see Supplementary Information for further discussion of the line shape). The third feature of the experiment is the electrical detection of the spin accumulation. This is done using the same tunnel interface, keeping the tunnel current, I , constant and recording the voltage, V , across the contact as B is changed ($V = V_{Si} - V_{FM}$, where V_{Si} and V_{FM} are, respectively, the potentials of the Si and the ferromagnetic electrode). For a linear response, the resulting voltage change, ΔV , is equal^{13,14} to $TSP \times \Delta\mu/2$, where TSP is the known^{15,16} tunnel spin polarization of the ferromagnet–insulator interface.

These three features are simultaneously required for a voltage signal to be observed. Hence, the room-temperature (300 K) data shown in Fig. 2b, c demonstrate electrical injection of spin polarization into (n-type) silicon from a ferromagnetic tunnel contact, the

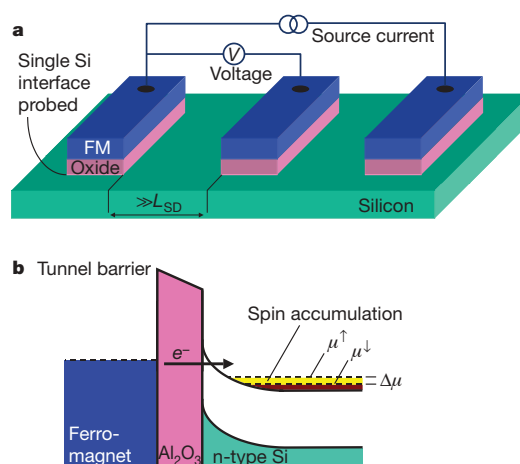


Figure 1 | Device geometry and energy diagram of magnetic contact with n-Si. **a**, Three-terminal device for injection and detection of spin polarization in Si under a single contact (left) consisting of an oxide insulator and a ferromagnetic-metal electrode (FM; blue). Contacts used to source current (right) and detect the voltage (middle) are placed away from the active interface by more than several spin diffusion lengths (L_{SD}). Each contact has an area of $100 \times 200 \mu\text{m}^2$. **b**, Energy band profile of the junction, depicting the ferromagnet, the Al_2O_3 barrier and the n-type Si conduction and valence bands bending up towards the oxide, forming a depletion region in the Si that acts as a second part of the tunnel barrier.

¹MESA⁺ Institute for Nanotechnology, University of Twente, 7500 AE Enschede, The Netherlands.

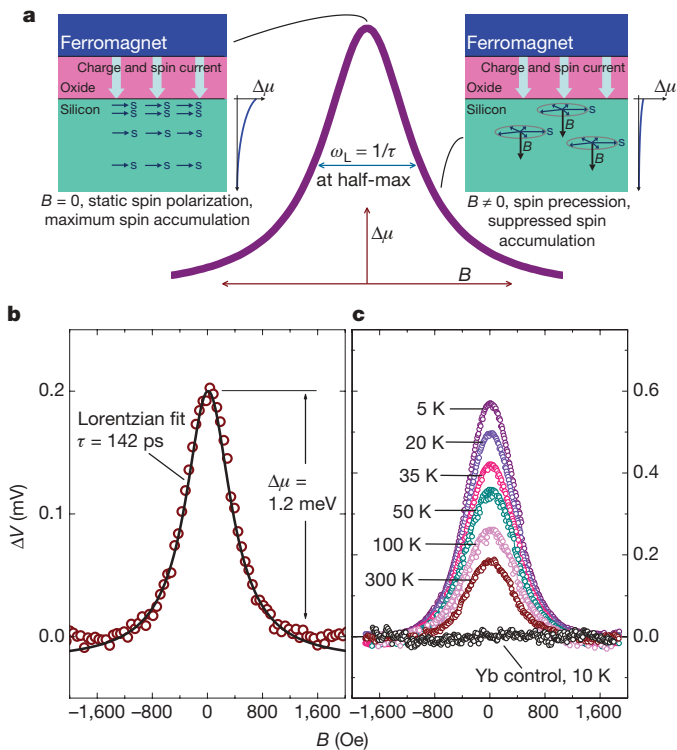


Figure 2 | Electrical injection and detection of a large spin accumulation in n-type Si at 300 K. **a**, Hanle effect, producing a decay of the net spin accumulation, $\Delta\mu$, due to spin precession in a magnetic field, B , perpendicular to the electron spins (s) in the Si. At constant current, a voltage change, ΔV , across the junction results. **b**, Detected ΔV across an n-Si–Al₂O₃–Ni₈₀Fe₂₀(5 nm)–Co(20 nm) tunnel junction at $T = 300$ K, as a function of magnetic field perpendicular to the interface. Data are taken with a constant source current of 734 μ A, corresponding to $V = +172$ mV at $B = 0$. The solid line is a Lorentzian fit with $\tau = 142$ ps. **c**, Detected ΔV for various temperatures, as indicated, for the same junction (for all curves, $V = +172$ mV at $B = 0$; the source current varied from 250 μ A (5 K) to 734 μ A (300 K)). Also shown (black symbols; +172 mV, 730 μ A) is data at 10 K for a control device with 2 nm of Yb inserted between the Al₂O₃ and the Ni₈₀Fe₂₀ in an otherwise identical junction. Measurement accuracy is represented by the size of the data symbols used.

Hanle precession of the electron spins in the silicon and the electrical detection of the spin accumulation. For constant tunnel current across an n-Si–Al₂O₃–Ni₈₀Fe₂₀ junction, we observe that the voltage decreases with increasing applied magnetic field as spin precession gradually reduces $\Delta\mu$ to zero. The signal is reasonably described by a Lorentzian line shape (solid line in Fig. 2b). The slight deviation at the highest B values is discussed in Supplementary Information. Similar data (Fig. 2c) were obtained over the full range of temperatures investigated, with ΔV being larger at low values of T .

Several arguments can be made to exclude the possibility of artefacts contributing to the signal. The resistances of the ferromagnetic metal and the Si between the two voltage probes contribute to the voltage, but they are at least two orders of magnitude smaller than the resistance of the tunnel barrier. The Si showed no significant magnetoresistance due to Lorentz deflection of the electrons by the applied magnetic field, which moreover would have produced a voltage increase as the magnetic field increased. Nevertheless, we performed a decisive test using a control device with 2 nm of non-magnetic Yb inserted between Al₂O₃ and Ni₈₀Fe₂₀ in an otherwise identical junction (Fig. 2c, black symbols). This is known¹⁷ to suppress the spin polarization of the injected tunnel current such that $\Delta\mu = 0$, which is what we observed. A similar null result for the Yb control device was obtained over the full range of T and V values investigated. This unambiguously proves that the observed signals are bona fide and represent spin accumulation induced by injection of a spin-polarized tunnel current.

Perhaps the most noteworthy feature is the clear and large spin accumulation observed at room temperature. The magnitude of the spin accumulation at the tunnel interface is obtained from $\Delta V = \text{TSP} \times \Delta\mu/2$, using the known^{15,16} TSP value, of 0.3, for Al₂O₃–Ni₈₀Fe₂₀ at 300 K. We then obtain $\Delta\mu = 1.2$ meV at 300 K, which is large. From the half-width of the Hanle curve (for which $\omega_L = 1/\tau$), we obtain the spin lifetime $\tau = 142$ ps for our heavily doped n-Si with a measured electron density of 1.8×10^{19} cm⁻³ at 300 K. Although there is no transport data available for comparison, electron spin resonance data^{18,19} and recent theory²⁰ give electron spin lifetimes of about 10 ns at 300 K for low-doped n-Si in which the Elliott–Yafet mechanism due to phonon scattering is dominant. Impurity scattering by the high density of donors in our samples is expected to reduce the spin lifetime. To first order, the spin relaxation time due to the Elliott–Yafet mechanism is given by $\tau_k/4\langle b^2 \rangle$, where τ_k is the momentum relaxation time and $\langle b^2 \rangle$ is the spin-mixing probability arising from the spin–orbit coupling of the electronic states ($\langle b^2 \rangle$ is about 4×10^{-6} for conduction-band electrons in Si at 300 K (ref. 20)). With the value of τ_k derived from the measured mobility (118 cm² V⁻¹ s⁻¹), this predicts a spin lifetime of about 1 ns, consistent with electron spin resonance data^{21,22} for heavily doped n-Si. Our measured value is smaller, suggesting that the spin lifetime is reduced in the proximity of the oxide interface and the ferromagnetic metal electrode. We note that, strictly speaking, we should consider the extracted spin lifetime of 142 ps as a lower bound (Supplementary Information).

We also obtain the spin diffusion length $L_{\text{SD}} = \sqrt{D\tau}$ in the Si, where D is the diffusion constant ($D = 3.7$ cm² s⁻¹ at 300 K as derived from the measured electron mobility). With $\tau = 142$ ps, we then obtain $L_{\text{SD}} = 230$ nm at room temperature for our heavily doped n-type Si. Such values are sufficient to transfer spin information over the typical length ($L < 100$ nm) of the channels of modern silicon transistors with only a modest decay of the spin accumulation.

Comparable data was reproducibly obtained from several devices prepared in different runs. Therefore, we can now systematically investigate the factors that control the spin accumulation. Let us first concentrate on n-type Si and examine the influence of the tunnel barrier, which has two parts: the Al₂O₃ tunnel barrier and the Schottky tunnel barrier in the Si due to carrier depletion near the oxide interface (Fig. 1b). The latter is 0.7–0.8 eV high and about 5 nm wide for the Si doping concentration used, making it transparent to tunnelling electrons. We examine whether the spin accumulation is influenced by the presence of this Schottky tunnel barrier by removing it and the associated depletion region by exposing the Si to a flux of Cs before preparation of the Al₂O₃ and the ferromagnetic electrode (Methods Summary). The Cs is known²³ to create states in the Si bandgap close to the conduction-band minimum. For Si–Al₂O₃–ferromagnet structures, this results in an almost flat band condition, as illustrated in the inset of Fig. 3, with a Schottky barrier height of less than 0.2 eV. When the Schottky tunnel barrier is suppressed with Cs, a clear Hanle signal is still observed (Fig. 3a, b). We find that at 300 K, the spin accumulations with and without Cs are of the same order of magnitude, and that the width of the Hanle curve is not changed. Both observations show that the spin accumulation at room temperature is robust and not drastically influenced by the Schottky tunnel barrier in the Si.

From the above result, we conclude that the large value of $\Delta\mu$ at 300 K represents the true spin accumulation in the Si. However, a different behaviour appears below 200 K. For junctions with Cs (no Schottky tunnel barrier), the spin signal changes only weakly with T (Fig. 3c) and the value of τ extracted from the width of the Hanle curve increases at low values of T (Fig. 3d). In sharp contrast, the junctions without Cs show an anomalous enhancement of the spin signal below 200 K, and a peculiar variation of τ , which does not increase at low T values. This anomalous behaviour below 200 K is probably due to two-step tunnelling through localized states at the oxide–semiconductor interface. This was recently proposed⁹ to explain the unexpected large

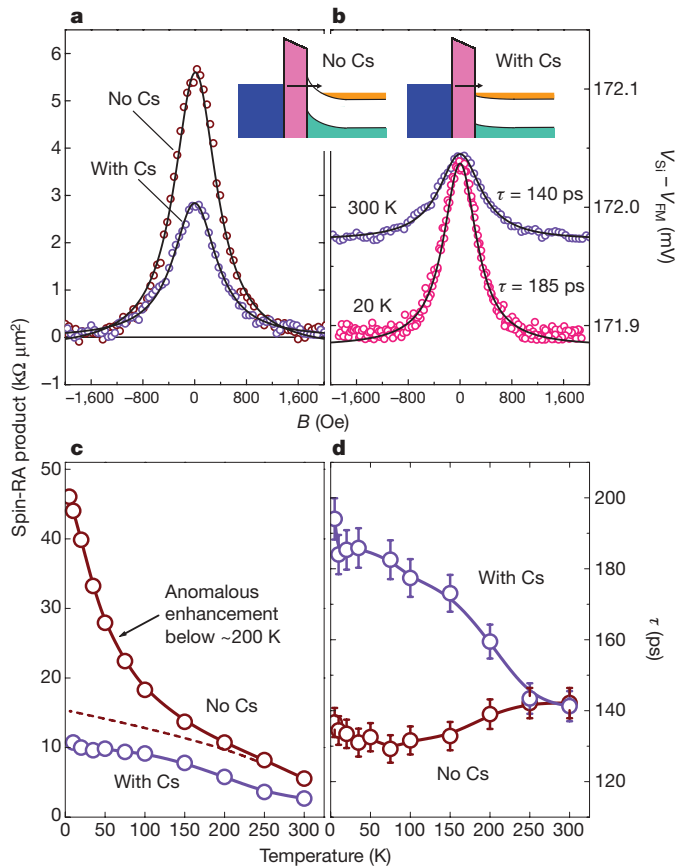


Figure 3 | Spin accumulation in n-type devices with the depletion region of the Si removed by Cs. **a**, Hanle signals at 300 K for junctions without Cs (same data as in Fig. 2) and with Cs, displayed as the spin-RA product. Data are taken with constant source currents of 511 μA and 734 μA for the junctions with and, respectively, without Cs, corresponding to about $V = +172$ mV at $B = 0$. **b**, Hanle curves with Cs at $T = 300$ K and $T = 20$ K. Solid lines are fits to Lorentzians with the τ values as indicated. Inset, energy-band profiles of the junctions with and without Cs. **c**, Spin-RA product versus T with and without Cs. The dashed line projects the expected signal without anomalous enhancement. **d**, The τ values extracted from Lorentzian fits versus T . Measurement accuracy is represented by the size of the data symbols used. Error bars define the range of τ values for which a reasonable fit of the Hanle curve is obtained.

spin signals observed in GaAs– Al_2O_3 –Co structures at low temperature. Compared with the semiconductor bulk, such localized states occupy a small volume and, for the same spin-injection current, support a larger spin accumulation as long as they are sufficiently decoupled from the conduction-band states in the Si bulk. This is the case for junctions without Cs, where a Schottky tunnel barrier separates the interface from the bulk. When the Schottky tunnel barrier is removed using Cs, the direct coupling between the interface and the bulk equalizes their spin accumulations, and the enhancement disappears. Hence, our experiments provide direct evidence for the importance of the proposed two-step tunnelling mechanism below 200 K.

The absence of any anomalous signal enhancement for the junctions with Cs (in which there is an Al_2O_3 tunnel barrier only) is evidence that in this case the true spin accumulation in the Si is obtained over the full temperature range. The spin signal, presented in Fig. 3c as the product of spin resistance, $\Delta V/I$, and area (the ‘spin-RA product’), should vary with T as $\tau \times \text{TSP}^2$, because $\Delta\mu$ scales with the TSP of the injected current and with τ , and another factor of TSP arises from the detection of the spin accumulation (from $\Delta V = \text{TSP} \times \Delta\mu/2$). Using the values of τ extracted from the width of the Hanle curve, and that fact that $\text{TSP} \propto (1 - \alpha T^{3/2})^{-1}$ with $\alpha = (3-5) \times 10^{-5} \text{K}^{-3/2}$ as previously determined²⁴, at low temperature we can expect the signal for the junctions

with Cs to increase by a factor of 2.5. This is not too different from the factor of four observed. The increase in the extracted τ values, from 140 ps at 300 K to about 190 ps at low temperature, is reasonable for a spin relaxation time^{20,21}. The conventional formula, $\tau_k/4\langle b^2 \rangle$, for spin relaxation due to the Elliott–Yafet mechanism predicts a modest increase at low temperature. The measured mobility (which is directly proportional to τ_k) changes by less than 5%, whereas $\langle b^2 \rangle$ was calculated²⁰ to decrease by 30–50% at low temperature. The observed increase in τ , of 35%, is consistent with this.

An important question is how large $\Delta\mu$ can be and how it varies with applied bias voltage (or current). We find (Fig. 4) that below 200 K, the spin-RA product is anomalously large owing to the contribution of two-step tunnelling through interface states, as discussed. Above 200 K, this contribution is negligible, and the data at 300 K is believed to represent the intrinsic behaviour. The spin-RA product at 300 K is asymmetric with respect to bias polarity, decreasing significantly for $V < 0$ for extraction of electrons from the Si, but depending only weakly on V for injection of electrons into the Si at $V > 0$ (note that the spin detection efficiency also varies with V). A constant spin-RA product (300 K and $V > 0$) implies that the induced spin accumulation scales linearly with current, reaching a maximum of $\Delta\mu \approx 2.9$ meV ($\Delta V = 0.43$ mV and $\text{TSP} = 0.3$) for the largest current (+1.5 mA). Assuming a parabolic conduction band and a Fermi–Dirac distribution for each spin, this translates into densities of $0.94 \times 10^{19} \text{cm}^{-3}$ and $0.86 \times 10^{19} \text{cm}^{-3}$ for majority and, respectively, minority spin electrons at room temperature and a sizeable electron spin polarization of 4.6% in the n-type Si.

Next we describe spin polarization in p-type Si at room temperature. The polarization is created in the valence band and the electronic carriers are holes. Results are shown in Fig. 5 for boron-doped p-type Si with a measured hole density of $4.8 \times 10^{18} \text{cm}^{-3}$ at 300 K. A clear Hanle signal is observed (Fig. 5a), demonstrating electrically induced spin polarization of holes in the valence band of p-type silicon, the spin precession of the holes and the electrical detection of the spin accumulation of holes. From the width of the Hanle curve, we extract a value of $\tau = 270$ ps for the hole spin lifetime at 300 K, which is larger than that for electrons in n-type Si (Fig. 2). Comparing with the conduction band, a stronger spin–orbit coupling strength in the Si valence band, and hence a smaller value of τ , might be expected. This is apparently compensated for by the density of acceptor impurities in the p-type sample being less than the donor impurity density in the n-type samples. We have used the free-electron g -factor, $g = 2$, also for valence band holes, in the absence of unique and accurate data²⁵. If the g -factor for holes is different, the value of τ has to be adjusted correspondingly. For $\tau = 270$ ps and the measured hole mobility of $117 \text{cm}^2 \text{V}^{-1} \text{s}^{-1}$ ($D = 3.6 \text{cm}^2 \text{s}^{-1}$), we obtain a hole

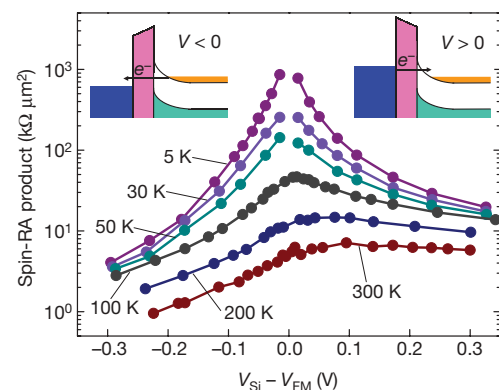


Figure 4 | Variation of spin signals with applied bias voltage in n-type Si devices. Spin-RA product as a function of applied bias voltage, V , at different temperatures, as indicated, for the same junction as in Fig. 2. For $V > 0$ and $V < 0$, spin-polarized electrons are injected into and, respectively, extracted from the Si conduction band, as sketched in the insets. Measurement accuracy is represented by the size of the data symbols used.

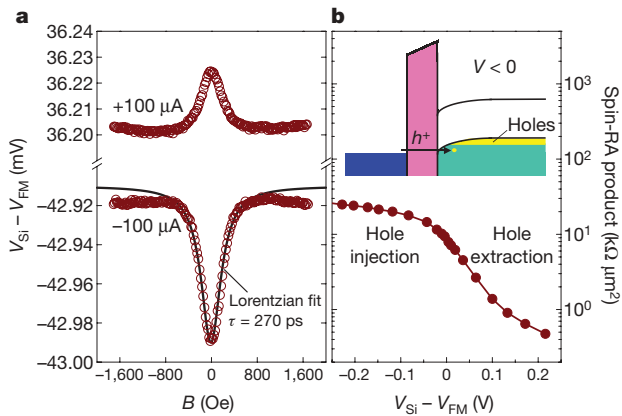


Figure 5 | Spin accumulation of holes in p-type Si at 300 K. **a**, Detected ΔV across a p-Si-Al₂O₃-Ni₈₀Fe₂₀ tunnel junction at $T = 300$ K, as a function of applied magnetic field, **B**. Data for the two curves are taken with a constant current of either $-100 \mu\text{A}$ or $+100 \mu\text{A}$, as indicated. The solid line is a Lorentzian fit with $\tau = 270$ ps. **b**, Spin-RA product versus applied bias voltage at 300 K. Inset, energy-band diagram for $V < 0$, in which spin-polarized holes (h^+) tunnel from the ferromagnetic metal into the valence band of the Si, where they are added to the pre-existing holes (yellow). This is equivalent to electrons tunnelling from filled states (green) in the Si valence band into empty states in the ferromagnetic metal. Measurement accuracy is represented by the size of the data symbols used.

spin diffusion length of $L_{\text{SD}} = 310$ nm at room temperature for our p-type Si. Figure 5b shows the variation of the spin-RA product with V for p-type devices. Just as for n-type Si, this product is nearly constant as a function of bias voltage for the polarity in which (hole) carriers are injected into the Si ($V < 0$ in this case), and exhibits a faster decay when the spin accumulation is created by extracting (hole) carriers from the Si ($V > 0$).

An elementary estimation of the steady state value of $\Delta\mu$, balancing the net amount of injected spins with an equal amount of spin flips in the Si per unit time^{13,14}, predicts a $\Delta\mu$ value about two orders of magnitude smaller than that observed. This may in part be due to a possible underestimation of the extracted spin lifetime (Supplementary information). However, we propose that another likely factor is the lateral inhomogeneity of the tunnel current. This is well known to exist in tunnel junctions as a result of the thickness and composition variations of the barrier. The real (local) tunnel current density that determines the spin accumulation may then be significantly larger than the average current density calculated from the geometric contact area.

The electrical creation and detection of a large and robust spin accumulation in Si at room temperature is a useful advance given the prevalence of Si in semiconductor technology. The scaling of $\Delta\mu$ with current density implies that even larger values should be feasible with optimized low-resistance contacts. Contact materials with larger TSP values can be used, and a larger spin lifetime may be obtained for Si with a lower doping density and/or optimized interfaces. This and other characteristics, and the fundamental rules that govern the behaviour of spin in Si devices at room temperature, can now be further explored.

METHODS SUMMARY

We fabricated the Si/Al₂O₃/ferromagnetic metal contacts on Si (100) substrates as previously described¹⁵. The n-type silicon-on-insulator wafer has a 5- μm thick active Si layer with As doping and a resistivity of 3 m Ωcm at 300 K. The p-type silicon-on-insulator wafer has a 3- μm thick active Si layer with B doping and a resistivity of 11 m Ωcm at 300 K. After surface treatment by hydrofluoric acid to remove oxide, the substrate was introduced into the load-lock chamber in which, if desired, it was exposed to Cs using a Cs alkali-metal dispenser²⁶ (SAES Getters). The current through the dispenser was increased in steps to 6 A in 18 min and kept at 6 A for another 15 min, and the pressure was constant at 10^{-7} mbar. After its transfer into the ultrahigh-vacuum chamber, we prepared the tunnel barrier by electron-beam deposition of Al₂O₃ (with nominal thicknesses of 0.5 nm for

n-type Si and 0.7 nm for p-type Si) from an Al₂O₃ single-crystal source, followed by plasma oxidation for 2.5 min and electron-beam deposition of the ferromagnetic-metal top electrode.

Received 2 August; accepted 8 October 2009.

- Žutić, I., Fabian, J. & Das Sarma, S. Spintronics: fundamentals and applications. *Rev. Mod. Phys.* **76**, 323–410 (2004).
- Chappert, C., Fert, A. & Nguyen van Dau, F. The emergence of spin electronics in data storage. *Nature Mater.* **6**, 813–823 (2007).
- Lou, X. *et al.* Electrical detection of spin transport in lateral ferromagnet-semiconductor devices. *Nature Phys.* **3**, 197–202 (2007).
- Appelbaum, I., Huang, B. & Monsma, D. J. Electronic measurement and control of spin transport in silicon. *Nature* **447**, 295–298 (2007).
- van't Erve, O. M. J. *et al.* Electrical injection and detection of spin-polarized carriers in silicon in a lateral transport geometry. *Appl. Phys. Lett.* **91**, 212109 (2007).
- Ando, Y. *et al.* Electrical injection and detection of spin-polarized electrons in silicon through Fe₃Si/Si Schottky tunnel barrier. *Appl. Phys. Lett.* **94**, 182105 (2009).
- Ciorga, M. *et al.* Electrical spin injection and detection in lateral all-semiconductor devices. *Phys. Rev. B* **79**, 165321 (2009).
- Lou, X. *et al.* Electrical detection of spin accumulation at a ferromagnet-semiconductor interface. *Phys. Rev. Lett.* **96**, 176603 (2006).
- Tran, M. *et al.* Enhancement of the spin accumulation at the interface between a spin-polarized tunnel junction and a semiconductor. *Phys. Rev. Lett.* **102**, 036601 (2009).
- Hanbicki, A. T., Jonker, B. T., Itskos, G., Kioseoglou, G. & Petrou, A. Efficient electrical spin injection from a magnetic metal/tunnel barrier contact into a semiconductor. *Appl. Phys. Lett.* **80**, 1240–1242 (2002).
- Motsnyi, V. F. *et al.* Electrical spin injection in a ferromagnet/tunnel barrier/semiconductor heterostructure. *Appl. Phys. Lett.* **81**, 265–267 (2002).
- Jonker, B. T., Kioseoglou, G., Hanbicki, A. T., Li, C. H. & Thompson, P. E. Electrical spin-injection into silicon from a ferromagnetic metal/tunnel barrier contact. *Nature Phys.* **3**, 542–546 (2007).
- Fert, A. & Jaffrès, H. Conditions for efficient spin injection from a ferromagnetic metal into a semiconductor. *Phys. Rev. B* **64**, 184420 (2001).
- Osipov, V. V. & Bratkovsky, A. M. Spin accumulation in degenerate semiconductors near modified Schottky contact with ferromagnets: spin injection and extraction. *Phys. Rev. B* **72**, 115322 (2005).
- Min, B. C., Motohashi, K., Lodder, J. C. & Jansen, R. Tunable spin-tunnel contacts to silicon using low-work-function ferromagnets. *Nature Mater.* **5**, 817–822 (2006).
- Park, B. G., Banerjee, T., Lodder, J. C. & Jansen, R. Tunnel spin polarization versus energy for clean and doped Al₂O₃ barriers. *Phys. Rev. Lett.* **99**, 217206 (2007).
- Patel, R. S., Dash, S. P., de Jong, M. P. & Jansen, R. Magnetic tunnel contacts to silicon with low-work-function ytterbium nanolayers. *J. Appl. Phys.* **106**, 016107 (2009).
- Lepine, D. J. Spin resonance of localized and delocalized electrons in phosphorus-doped silicon between 20 and 300 K. *Phys. Rev. B* **2**, 2429–2439 (1970).
- Fabian, J., Matos-Abiague, A., Ertler, C., Stano, P. & Žutić, I. Semiconductor spintronics. *Acta Phys. Slov.* **57**, 565–907 (2007).
- Cheng, J. L., Wu, M. W. & Fabian, J. Theory of the spin relaxation of conduction electrons in silicon. Preprint at (<http://arxiv.library.cornell.edu/abs/0906.4054>) (2009).
- Kodera, H. Effect of doping on the electron spin resonance in phosphorus doped silicon. II. *J. Phys. Soc. Jpn* **21**, 1040–1045 (1966).
- Anderberg, J. M., Einevoll, G. T., Vier, D. C., Schultz, S. & Sham, L. J. Probing the Schottky barrier with conduction electron spin resonance. *Phys. Rev. B* **55**, 13745–13751 (1997).
- Biagi, R. *et al.* Photoemission investigation of alkali-metal-induced two-dimensional electron gas at the Si(111)(1 \times 1):H surface. *Phys. Rev. B* **67**, 155325 (2003).
- Shang, C. H., Nowak, J., Jansen, R. & Moodera, J. S. Temperature dependence of magnetoresistance and surface magnetization in ferromagnetic tunnel junctions. *Phys. Rev. B* **58**, R2917–R2920 (1998).
- Feher, G., Hensel, J. C. & Gere, E. A. Paramagnetic resonance absorption from acceptors in silicon. *Phys. Rev. Lett.* **5**, 309–311 (1960).
- Succi, M., Canino, R. & Ferrario, B. Atomic-absorption evaporation flow-rate measurements of alkali metal dispensers. *Vacuum* **35**, 579–582 (1985).

Supplementary Information is linked to the online version of the paper at www.nature.com/nature.

Acknowledgements This work was financially supported by the NWO-VIDI programme and the Netherlands Foundation for Fundamental Research on Matter.

Author Contributions S.P.D. fabricated most of the devices and carried out most of the measurements. S.S. and M.P.d.J. contributed to the device fabrication and some of the measurements. R.S.P. contributed to the Yb control experiment. All co-authors contributed important insights and ideas. R.J. supervised and coordinated the research. R.J. and S.P.D. wrote the paper, with help from all co-authors.

Author Information Reprints and permissions information is available at www.nature.com/reprints. Correspondence and requests for materials should be addressed to R.J. (ron.jansen@el.utwente.nl).